

# Extensional flows with viscous heating

By JONATHAN J. WYLIE<sup>1</sup> AND HUAXIONG HUANG<sup>2</sup>

<sup>1</sup>Department of Mathematics, City University of Hong Kong, Kowloon, Hong Kong

<sup>2</sup>Department Mathematics and Statistics, York University, Toronto, Ontario,  
Canada M3J 1P3

(Received 30 May 2006 and in revised form 6 September 2006)

In this paper we investigate the role played by viscous heating in extensional flows of viscous threads with temperature-dependent viscosity. We show that there exists an interesting interplay between the effects of viscous heating, which accelerates thinning, and inertia, which prevents pinch-off. We first consider steady drawing of a thread that is fed through a fixed aperture at given speed and pulled with a constant force at a fixed downstream location. For pulling forces above a critical value, we show that inertialess solutions cannot exist and inertia is crucial in controlling the dynamics. We also consider the unsteady stretching of a thread that is fixed at one end and pulled with a constant force at the other end. In contrast to the case in which inertia is neglected, the thread will always pinch at the end where the force is applied. Our results show that viscous heating can have a profound effect on the final shape and total extension at pinching.

---

## 1. Introduction

Viscous heating plays an important role in a number of applications and is particularly relevant to the polymer processing industry. Many of the fluids used in such applications have a viscosity that varies rapidly with temperature and this can give rise to strong feedback effects that can lead to profound changes in the flow structure. Pearson (1977) and Ockendon (1979) showed that viscous heating could lead to plug flows in channels. In recent years there has been a renewed interest in viscous heating as a number of authors have shown that its effects can dramatically destabilize viscous flows (Al-Mubaiyedh, Sureshkumar & Khomani 2002; White & Muller 2002). Vasilyev, Ten & Yuen (2001) have shown that viscous gravity currents can propagate faster as a result of viscous heating. Costa & Macedonio (2005) have shown that interesting secondary flows can be triggered in channel flows.

In this paper, we examine two distinct types of extensional flow that are motivated by two specific examples. In both cases, we show that apparently weak viscous heating can have a dramatic effect on the dynamics. The analysis that we present in this paper is quite general and can be applied to a number of situations in which threads are subjected to extensional forces.

The first type of flow is that of a thread that is fed into an apparatus at a fixed speed and is pulled at a fixed downstream location. This is a widely used industrial method to produce textile threads from polymeric materials and optical fibres from molten glass. This type of fibre stretching has been very widely studied in the isothermal case and we refer the reader to a comprehensive review by Denn (1980) for further details. Matsumoto & Bogue (1978) conducted experiments with a material whose viscosity varied rapidly with temperature. They found stretching was extremely unstable and

noted that this sensitivity cannot be explained using a traditional isothermal analysis. For high-speed optical fibre pulling, Yin & Jaluria (2000) showed that the heat generated by viscous dissipation can become important in the regions in which rapid thinning occurs, but their study focused on other factors that can affect the manufacturing process. Simple order-of-magnitude estimates often indicate that the effects of viscous heating are small, and to our knowledge the effect of viscous heating in the pulling of viscous threads has received relatively little attention. In the extension of threads, inertia is also frequently neglected, although it can become important in some situations, as shown by Wilson (1988), Kaye (1991) and Stokes & Tuck (2004). However, we show that even apparently very weak viscous heating effects can lead to dramatic changes in the flow structure and, as a result, inertia becomes important. By deriving exact solutions, we show that inertialess solutions can only exist for values of the pulling force below a critical value. Beyond this critical value inertia cannot be neglected since it is crucial in controlling the flow.

The second type of flow is that of a thread that is fixed at one end and pulled at the other end with a fixed force. This type of flow is important in the production of tapered glass fibres for optical microscopy (Gallacchi *et al.* 2001) and is an integral part of the manufacture of glass microelectrodes (Huang *et al.* 2003). Here, a glass tube is extended to form an electrode with the required tip size and shape. In the latter stages of the pulling, the extensional velocity increases dramatically during stretching, and can result in a large strain rate and significant viscous heating. If inertia is neglected, we derive exact solutions and show that the location at which pinching occurs is determined by the initial conditions. The total extension at pinching is unbounded in the absence of viscous heating, but is finite for any non-zero rate of viscous heating. If inertia is included, we show that the thread always pinches at the location where the force is applied for both zero and non-zero viscous heating. Nevertheless, viscous heating can have a dramatic effect on the final shape and the total extension at pinching.

## 2. Model for thread pulling

We consider an axisymmetric thread with a cross-sectional area  $A'$ , velocity  $u'$ , and temperature  $\theta'$ . We define  $x'$  as the distance along the thread measured from a fixed reference point and  $t'$  as the time. We denote the density of the fluid as  $\rho$ , the specific heat capacity as  $c_p$  and the surface tension coefficient as  $\gamma$ . The thread is pulled by an external force  $F$ , has characteristic cross-sectional area  $A_0$ , length  $L$ , temperature  $\theta_0$ , thermal conductivity  $k$ , emissivity  $\alpha$  and viscosity  $\mu_0$ .

The viscosity of many of the materials used in such extensional flows can vary dramatically with temperature. For example, the glass used to produce electrodes typically requires a temperature change of order 50 K to cause a significant change in the viscosity (Huang *et al.* 2003). We denote this characteristic temperature change as  $\Theta$ . Typical thermal expansion coefficients for glass and polymeric materials are of the order of  $10^{-5} \text{ K}^{-1}$  (Encyclopedia Britannica; see also Scholze; 1990, §3.2) and so for temperature changes of order 50 K, the material can be approximated well as having constant density. Moreover, for glass materials, the typical value of surface tension is of order  $0.1 \text{ kg s}^{-2}$ , whereas the coefficient describing the magnitude of changes in surface tension with respect to temperature is of order  $4 \times 10^{-5} \text{ kg s}^{-2} \text{ K}^{-1}$  (Scholze, 1990, p. 327). Therefore, for temperature changes of order 50 K, we will also assume that the surface tension coefficient is constant.

For large aspect ratio,  $\delta = A_0/L^2 \ll 1$ , the governing equations for laminar, axisymmetric and incompressible extensional flow have been derived by a number of authors, see for example Forest, Zhou & Wang (2000), Yin & Jaluria (2000) and Fitt *et al.* (2001). Using the natural scales

$$u' = FL(3\mu_0 A_0)^{-1}u, \quad A' = A_0 A, \quad x' = Lx, \quad t' = 3\mu_0 A_0 F^{-1}t, \quad \theta' = \theta_0 + \Theta\theta,$$

the long-wavelength dimensionless equations representing the conservation of mass and momentum are

$$A_t + (uA)_x = 0, \quad (2.1)$$

$$R \left( \frac{\partial u}{\partial t} + u \frac{\partial u}{\partial x} \right) = \frac{1}{A} \frac{\partial}{\partial x} \left( \mu A \frac{\partial u}{\partial x} + \lambda \sqrt{A} \right), \quad (2.2)$$

where

$$R = \frac{\rho FL^2}{9\mu_0^2 A_0}, \quad \lambda = \frac{\gamma \sqrt{\pi A_0}}{F}.$$

If the Biot number

$$B = \frac{\alpha k_b \theta_0^4 A_0^{1/2}}{k\Theta}$$

is small then the heat equation is given by Forest *et al.* (2000):

$$\theta_t + u\theta_x = \mathcal{H} \mu u_x^2 - CA^{-1/2} + Pe^{-1} \frac{1}{A} \frac{\partial}{\partial x} \left( A \frac{\partial \theta}{\partial x} \right), \quad (2.3)$$

where  $k_b$  is the Boltzmann constant, and

$$\mathcal{H} = \frac{F}{\rho c_p \Theta A_0}, \quad Pe = \frac{L^2 F \rho c_p}{k \mu_0 A_0}, \quad C = \frac{B}{\delta Pe}.$$

We will adopt the exponential viscosity law that, in dimensionless form, is given by

$$\mu(\theta) = \exp(-\theta). \quad (2.4)$$

This viscosity law can give excellent agreement with experimental data for viscosity variations in excess of five orders of magnitude (Huang *et al.* 2003). In dimensionless form, the boundary condition at the location where the force is applied is given by

$$\mu A u_x + \lambda A^{1/2} = 1. \quad (2.5)$$

The parameter values can vary widely depending on the particular industrial process, but we present order-of-magnitude estimates that are appropriate for optical fibre tip production and electrode pulling (Gallacchi *et al.* 2001; Huang *et al.* 2003). These are  $L \sim 10^{-2}$  m,  $A_0 \sim 10^{-6}$  m,  $F \sim 1$  N,  $\rho \sim 10^3$  kg m<sup>-3</sup>,  $c_p \sim 10^3$  J K<sup>-1</sup> kg<sup>-1</sup>,  $k \sim 1$  W m<sup>-1</sup> K<sup>-1</sup>,  $k_b = 5.7 \times 10^{-8}$  W m<sup>-2</sup> K<sup>-4</sup>,  $\theta_0 \sim 800$  K,  $\Theta \sim 50$  K,  $\gamma \sim 10^{-1}$  kg s<sup>-2</sup>,  $\alpha \sim 0.4$ , and  $\mu_0 \sim 10^4$  kg m s<sup>-1</sup>. These scales give  $B \sim 10^{-1}$ ,  $\delta \sim 10^{-2}$ ,  $R \sim 10^{-4}$ ,  $\lambda \sim 10^{-4}$ ,  $\mathcal{H} \sim 10^{-2}$ ,  $C \sim 10^{-3}$  and  $Pe \sim 10^4$ . Therefore, at first sight, inertia, surface tension, viscous heating, radiative heat losses and axial conduction are all small and this has led many authors to neglect all of these effects. However, one must take care that these estimates are still appropriate if the thread becomes thin. For a fixed applied force, (2.5) indicates that as  $A$  becomes small,  $u_x$  can increase sufficiently that the viscous stress  $\mu A u_x$  can have the same magnitude as the applied force. However, as  $A$  becomes small the surface tension term  $\lambda A^{1/2}$  must decrease in importance. Since the surface tension is initially small, we are therefore justified in neglecting surface tension.

Similarly, as  $A$  decreases, (2.3) and (2.5) show that the advective term increases as  $A^{-1}$  whereas the radiative cooling term increases more slowly as  $A^{-1/2}$ . Therefore, as  $A$  decreases, the radiative cooling becomes less important than the advection term and we therefore neglect radiative cooling. The axial conduction can also be neglected as it is small initially and remains small during stretching. In contrast, the values of  $\mathcal{H}$  and  $R$  are typically small, but if the thread thins significantly, we will show that the effects of viscous heating and inertia will become important.

In the following, we will consider two related problems that share a number of similar features. As described in §1 the first problem is motivated by continuous drawing with a constant feeding rate, whereas the second problem is motivated by the unsteady extension of a thread. The first problem has steady states and these allow us to gain important insights into the role of inertia in the second problem.

### 3. Steady drawing

We consider a device that feeds a cylindrical thread of viscous fluid through a fixed aperture with cross-sectional area  $A_0$  at speed  $u_0$  of order  $1 \text{ m s}^{-1}$ . At a position  $L$  downstream a fixed force  $F$  is applied that stretches the thread.

The dimensionless equations are given by (2.1)–(2.3) with  $C = 0$ ,  $\lambda = 0$  and  $Pe^{-1} = 0$ . The boundary condition at the exit,  $x = 1$ , is given by (2.5) with  $\lambda = 0$ . The boundary conditions at the entry,  $x = 0$ , are  $A = 1$ ,  $\theta = 0$  and  $\mathcal{F}u = 1$ , where

$$\mathcal{F} = \frac{FL}{3\mu_0 A_0 u_0} \quad (3.1)$$

measures the degree of thinning experienced by a constant-viscosity thread whilst it remains in the domain. Small values of  $\mathcal{F}$  imply that the thread passes through the device sufficiently quickly that it is thinned weakly by the imposed force, whereas large values of  $\mathcal{F}$  imply that the thread will experience significant thinning.

If we consider steady states, the equation of conservation of mass can be integrated along with the boundary conditions at  $x = 0$  to yield

$$\mathcal{F}uA = 1. \quad (3.2)$$

Using (3.2) to eliminate  $A$  from the time-independent version of (2.2), integrating and applying the boundary condition (2.5) at  $x = 1$  yields

$$u_x = \mu^{-1}u[\mathcal{F} - R(u(1) - u)], \quad (3.3)$$

where  $u(1)$  is the velocity at the exit which must be solved for. Substituting (3.3) into the time-independent version of the heat equation (2.3) with  $C = 0$  and  $Pe^{-1} = 0$  yields

$$\theta_x = \mu^{-1}\mathcal{H}u[\mathcal{F} - R(u(1) - u)]^2. \quad (3.4)$$

Dividing (3.4) by (3.3), integrating and applying the boundary condition at  $x = 0$  gives

$$\theta = \mathcal{H}[(\mathcal{F} - Ru(1))(u - \mathcal{F}^{-1}) + \frac{1}{2}R(u^2 - \mathcal{F}^{-2})]. \quad (3.5)$$

Substituting (2.4) and (3.5) into (3.3), integrating and applying the boundary condition at  $x = 0$  yields

$$\int_1^{\mathcal{F}u} \frac{\exp(-\mathcal{H}[(1 - \mathcal{P}D_r)(v - 1) + \frac{1}{2}\mathcal{P}(v^2 - 1)])}{v[(1 - \mathcal{P}D_r) + \mathcal{P}v]} dv = \mathcal{F}x, \quad (3.6)$$

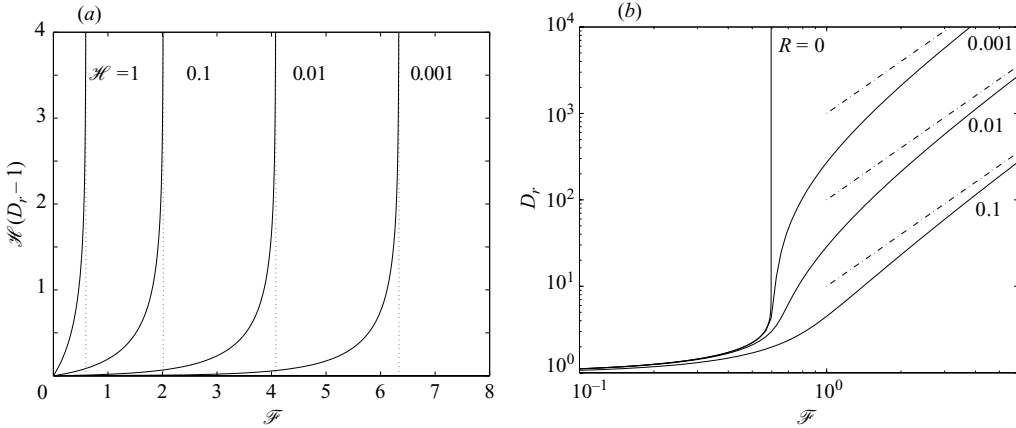


FIGURE 1. Steady drawing. (a) The scaled draw ratio  $\mathcal{H}(D_r - 1)$  vs.  $\mathcal{F}$  for  $R = 0$  for various values of  $\mathcal{H}$ . The dotted lines show the critical value of  $\mathcal{F}$  above which no steady solutions exist for  $R = 0$ . (b) The draw ratio vs.  $\mathcal{F}$  on a log-log scale for  $\mathcal{H} = 1$  and various values of  $R$ . The dashed-dotted lines represent the large- $\mathcal{F}$  asymptotic limit.

where  $D_r = u(1)/u(0) = \mathcal{F}u(1)$  is the draw ratio and

$$\mathcal{P} \equiv R\mathcal{F}^{-2} = \frac{\rho A_0 u_0^2}{F} \tag{3.7}$$

is the ratio of the flux of momentum from feeding to the stretching force. For the parameter values used in §2,  $\mathcal{F} \sim 0.3$  and  $\mathcal{P} \sim 10^{-3}$ . In order to evaluate the integrals in (3.6) one needs to know  $D_r$ . This can be obtained by using the condition  $\mathcal{F}u = D_r$  at  $x = 1$  to obtain

$$\int_1^{D_r} \frac{\exp(-\mathcal{H} [(1 - \mathcal{P}D_r)(v - 1) + \frac{1}{2}\mathcal{P}(v^2 - 1)])}{v[(1 - \mathcal{P}D_r) + \mathcal{P}v]} dv = \mathcal{F}. \tag{3.8}$$

For any parameter values this can be solved numerically for  $D_r$  using straightforward quadrature and Newton–Raphson methods. However, since  $\mathcal{P}$  is small we begin by setting it to zero which corresponds to neglecting inertia. In this case, the integral (3.6) can be computed without first computing  $D_r$  and the solution is given by

$$E_1(\mathcal{F}\mathcal{H}u) = E_1(\mathcal{H}) - \mathcal{F}e^{-\mathcal{H}x}, \tag{3.9}$$

where  $E_1$  is the exponential integral

$$E_1(u) = \int_u^\infty \frac{e^{-v}}{v} dv. \tag{3.10}$$

We can therefore obtain the draw ratio  $D_r$  as a function of  $\mathcal{F}$  by solving

$$E_1(\mathcal{H}D_r) = E_1(\mathcal{H}) - \mathcal{F}e^{-\mathcal{H}}. \tag{3.11}$$

This is plotted in figure 1(a). We immediately see that as  $\mathcal{F}$  approaches a critical value from below,  $D_r$  tends to infinity. For values of  $\mathcal{F}$  above the critical value, no steady-state solutions exist. The critical value,  $\mathcal{F}_c = e^{\mathcal{H}} E_1(\mathcal{H})$  can be obtained by letting  $D_r \rightarrow \infty$  in (3.11).

For sufficiently small  $\mathcal{F}$ , the amount of stretching that can occur before material elements exit the device is small. Therefore the heat generated by viscous heating will only weakly affect the viscosity and solutions will be close to the isothermal case. As

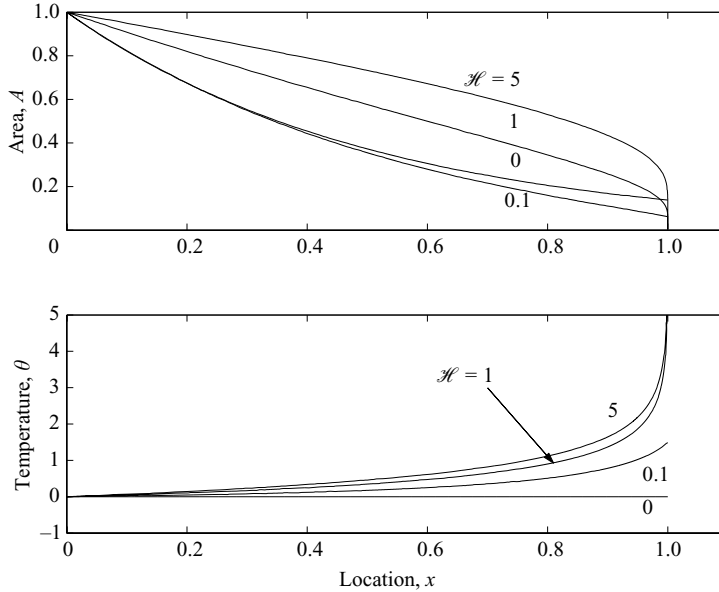


FIGURE 2. The cross-sectional area and temperature profiles for  $R = 0.01$  and  $\mathcal{F} = 2$  and various values of  $\mathcal{H}$ .

$\mathcal{F}$  is increased, the amount of stretching increases and causes extra viscous heating which makes the viscosity decrease and hence reduces the resistance to stretching. This allows more stretching to occur which generates more heat and so can lead to a runaway effect.

When  $\mathcal{H} \rightarrow 0$ , the critical value  $\mathcal{F}_c \rightarrow \infty$  and so the runaway phenomenon disappears. However, we note that as  $\mathcal{H} \rightarrow 0$  the critical value of  $\mathcal{F}$  tends to infinity very slowly as  $\mathcal{F}_c = O(\ln(1/\mathcal{H}))$ . Therefore, even apparently very small values of the parameter  $\mathcal{H}$  can still give rise to this runaway phenomenon at relatively moderate values of  $\mathcal{F}$ .

In practice such runaway effects will be saturated in one of two ways: either the temperature will increase sufficiently that the exponential viscosity law (2.4) will not be valid or alternatively inertia will become important. In this paper we will focus on the role of inertia, since treatment of the former case is straightforward.

In figure 1(b) we present the results of numerical integration of (3.8) that show how inertia modifies the dynamics. When  $\mathcal{F}$  is below the critical value, inertia plays a weak role in modifying the draw ratio. For values of  $\mathcal{F}$  above the critical value, inertia becomes crucial. The draw ratio is an increasing function of  $\mathcal{F}$ , and  $D_r \rightarrow \mathcal{F}^2/R$  as  $\mathcal{F} \rightarrow \infty$ . This corresponds to the case in which the thermal runaway is very strong and so the viscous resistance to stretching is small. In this case, the draw ratio is inertially controlled. In figure 2 we present the cross-sectional area and temperature profiles for a fixed value of  $\mathcal{F}$ , a fixed small value of  $R$  and varying values of  $\mathcal{H}$ . As the heating rate increases, the critical value of  $\mathcal{F} = \mathcal{F}_c$ , for which inertialess solutions can exist, decreases. When the heating rate is small ( $\mathcal{H} = 0.1$ ), inertialess solutions can exist and are similar to the  $\mathcal{H} = 0$  situation with slightly increased thinning due to the viscous heat generation. However, for the sufficiently large values of  $\mathcal{H} = 1$  or  $5$ , inertialess solutions do not exist. In this case, the solutions thin very rapidly near the exit and experience much weaker thinning over the bulk of the thread. The

role of inertia can be understood by considering equation (3.3). This equation shows how the effective pulling force, which we define to be  $\mathcal{F} - R(u(1) - u)$ , is reduced by inertia. At the exit of the device the force is prescribed. Near the exit,  $u$  is close to  $u(1)$ , and so inertia plays a weak role. Since viscous heating can lead to very small values of the viscosity, very rapid thinning can occur near the exit. On moving away from the exit, part of the force is required to accelerate the thread. This reduces the effective force on moving away from the exit and thus leads to weaker thinning in the bulk.

#### 4. Extension of thread with fixed force

We now turn our attention to the case of a thread that is fixed at one end and pulled with a constant force at the other end. As shown in Stokes & Tuck (2004), the system of equations becomes significantly simpler if expressed in Lagrangian coordinates  $(\xi, \tau)$ . The relationship between the Eulerian coordinates  $(x, t)$  and the Lagrangian coordinates  $(X, \tau)$  is given by  $\tau = t$  and  $X_\tau = u$ . This implies that the Lagrangian variable  $X$  is the spatial coordinate of a material point that was at the location  $x = \xi$  at the initial time  $\tau = 0$ .

In Lagrangian coordinates, (2.1) becomes  $(AX_\xi)_\tau = 0$ . Integrating and applying the initial conditions  $A(\xi, 0) = A_i(\xi)$  and  $X(\xi, 0) = \xi$ , gives  $X_\xi = A_i/A$ , and the total extension of the thread at time  $\tau$  is given by

$$X(1, \tau) = \int_0^1 \frac{A_i(\xi)}{A(\xi, \tau)} d\xi. \tag{4.1}$$

Equations (2.1)–(2.3) with  $C = 0$  and  $Pe^{-1} = 0$  become

$$A_\tau = -\frac{A^2 u_\xi}{A_i}, \tag{4.2}$$

$$RA_i u_\tau = \left[ \frac{\mu A^2 u_\xi}{A_i} \right]_\xi, \tag{4.3}$$

$$\theta_\tau = \mathcal{H} \frac{\mu(\theta) A^2 u_\xi^2}{A_i^2}. \tag{4.4}$$

The boundary conditions are  $u = 0$  at  $\xi = 0$  and  $\mu A^2 u_\xi / A_i = 1$  at  $\xi = 1$ . The initial conditions are  $u = 0$ ,  $\theta = \theta_i(\xi)$  and  $A = A_i(\xi)$  at  $\tau = 0$ .

##### 4.1. Zero viscous heating

If we neglect both viscous heating and inertia, then equations (4.2)–(4.4) can readily be solved to obtain

$$A = A_i(\xi) - \tau / \mu_i(\xi). \tag{4.5}$$

Therefore, pinching occurs at  $\tau_p = \min_\xi \{\mu_i A_i\}$  at the location  $\xi = \xi_p$ . Since we are using the long-wavelength approximation we will assume that  $A_i$  and  $\theta_i$  have continuous second derivatives. If the thread does not pinch at one of the end points, that is  $\xi_p \in (0, 1)$ , then since  $\xi_p$  is a minimum of  $\mu_i A_i$ , we have  $(\mu_i A_i)'|_{\xi_p} = 0$  and generically,  $(\mu_i A_i)''|_{\xi_p} > 0$ . Therefore, as time approaches the pinching time, the total extension is dominated by the contribution to the integral (4.1) near  $\xi = \xi_p$ .

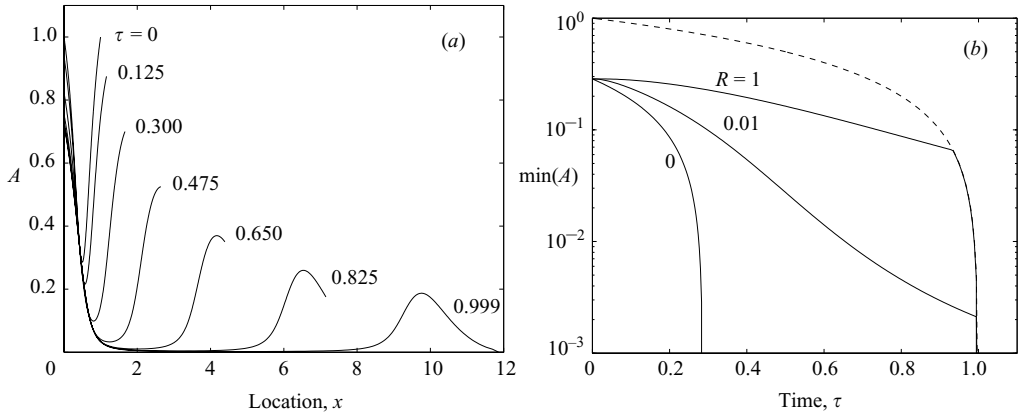


FIGURE 3. Stretching without viscous heating ( $\mathcal{H} = 0$ ). (a) The cross-sectional area vs.  $x$  at various times for  $R = 0.1$ . Pinching occurs at the end point at  $\tau = 1$ . (b) The minimum area vs. time for various values of  $R$ . The dotted line represents the area at the end point. The initial condition is given by (4.8) with  $K = 10$ .

Asymptotically, we obtain

$$X(1, \tau) \sim \frac{\sqrt{2}\pi\tau_p}{\sqrt{(\mu_i A_i)'|_{\xi_p}(\tau_p - \tau)}}. \tag{4.6}$$

If the thread pinches at one of the end points a similar calculation shows that, generically,

$$X(1, \tau) \sim \left| \frac{\tau_p \ln(\tau_p - \tau)}{(\mu_i A_i)'|_{\xi_p}} \right|. \tag{4.7}$$

In both cases, the total extension of the thread tends to infinity as the pinching time is approached. As the area tends to zero, the velocity tends to infinity and so we expect inertial terms to become important. When inertial terms are retained we were unable to obtain a general analytic solution, but an exact solution can be obtained for the area at the end at which the force is applied. This is because the force is prescribed at the end and so the inertial terms do not reduce the effective pulling force. Hence, (4.2) can be used to rewrite the applied force boundary condition as  $A_\tau = -1/\mu_i(1)$  at  $\xi = 1$ . Integrating with respect to  $\tau$  and applying the initial condition we obtain  $A(1, \tau) = A_i(1) - \tau/\mu_i(1)$ . Results obtained using a standard explicit time-stepping technique are shown in figure 3(a). For the examples presented in this paper we take the simple initial condition given by

$$\theta_i = 0, \quad A_i = \frac{1}{1 + K(\frac{1}{2})^2} + \frac{K(\xi - \frac{1}{2})^2}{1 + K(\xi - \frac{1}{2})^2} \tag{4.8}$$

that is symmetric about  $\xi = 1/2$  and has unit area at the end points  $\xi = 0$  and  $\xi = 1$ . We note that other initial conditions give similar behaviour. Although in applications,  $R$  is typically of the order of  $10^{-4}$ , for purposes of visualization, we use somewhat larger values of  $R$ .

If  $R$  is small, then initially the inertial correction to the effective pulling force is small and so the solution will be approximated well by (4.5). Therefore, the area decreases at an approximately uniform rate at all  $x$  locations. However, when the area becomes small the inertial terms become important. Our numerical results show that

inertia prevents pinching in the middle of the thread and the thread always pinches at the end point where the force is applied. The area remains bounded away from zero everywhere except at the end point, so the total extension (4.1) can diverge only if the contribution from the neighbourhood of  $\xi = 1$  diverges. In order to investigate the local behaviour one can consider the similarity solution of the form  $A = A(1, \tau)a(\eta)$ , where  $\eta = (1 - \xi)A_i(1)R^{1/2}/[\mu_i(1)A(1, \tau)^{3/2}]$ . Then, at leading order equations (4.2)–(4.4) give  $2a^2a'' - 3\eta a' + 2a = 0$  with boundary conditions  $a(0) = 1$  and  $a'(\infty) = 0$ . This similarity solution remains bounded away from zero and so the contribution to (4.1) near  $\xi = 1$  is of order  $\mu_i(1)R^{-1/2}A(1, \tau)^{1/2}$ . So near pinching,  $A(1, \tau) \rightarrow 0$ , the extension will remain finite.

In figure 3(b) we show the result of pulling a thread that has an initial profile given by (4.8). We plot the minimum area and the area at the end of the thread against time for different values of  $R$ . For  $R = 0$  the thread pinches in the middle, whereas for  $R \neq 0$  the area in the middle thins to a small value, but is ultimately overtaken by the value at the end point. The thread pinches at the end point in a finite time.

#### 4.2. The role of viscous heating

We now consider the effects of viscous heating on the pulled thread. Initially the inertial terms are small and therefore we neglect them. Equation (4.3) can be integrated to give

$$\mu A^2 u_\xi = A_i. \tag{4.9}$$

We can therefore eliminate  $u$  from equations (4.2) and (4.4) to obtain

$$\mu A_\tau = -1, \tag{4.10}$$

$$\mu A^2 \theta_\tau = \mathcal{H}. \tag{4.11}$$

Dividing (4.11) by (4.10), integrating and applying the initial condition yields

$$\theta - \theta_i = \mathcal{H}(A^{-1} - A_i^{-1}). \tag{4.12}$$

Substituting into (4.10), integrating and using the initial condition gives

$$\frac{A}{\mathcal{H}} e^{-\mathcal{H}/A} - E_1\left(\frac{\mathcal{H}}{A}\right) = -e^{-\mathcal{H}/A_i + \theta_i} \frac{\tau}{\mathcal{H}} + \frac{A_i}{\mathcal{H}} e^{-\mathcal{H}/A_i} - E_1\left(\frac{\mathcal{H}}{A_i}\right). \tag{4.13}$$

The solution is shown in figure 4(a). One can clearly see that the viscous heating leads the pinching to become highly localized.

The cross-sectional area  $A$  will go to zero at time

$$\tau_p = \min_\xi \left\{ e^{-\theta_i} \left[ A_i - \mathcal{H} e^{\mathcal{H}/A_i} E_1\left(\frac{\mathcal{H}}{A_i}\right) \right] \right\}. \tag{4.14}$$

When the thread is close to pinching, that is  $A \ll 1$ , (4.13) can be approximated by

$$\frac{A^2}{\mathcal{H}} e^{-\mathcal{H}/A} = e^{-\mathcal{H}/A_i + \theta_i} (\tau_p - \tau). \tag{4.15}$$

We can therefore see that  $A \rightarrow 0$  as  $-\mathcal{H}/\ln(\tau_p - \tau)$  as  $\tau \rightarrow \tau_p$ . In this case, in order to determine the total extension of the thread we define

$$p(\xi) = e^{-\theta_i} \left[ A_i - \mathcal{H} e^{\mathcal{H}/A_i} E_1\left(\frac{\mathcal{H}}{A_i}\right) \right]. \tag{4.16}$$

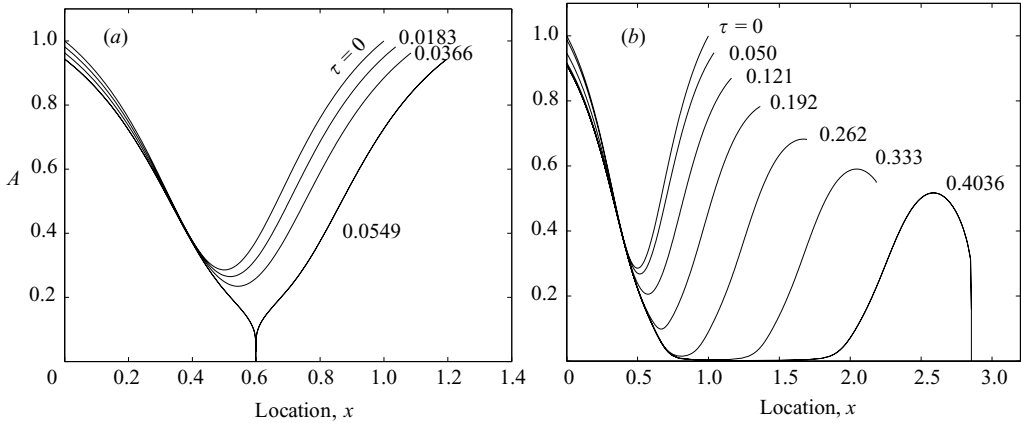


FIGURE 4. Pulling with viscous heating ( $\mathcal{H} = 1$ ). The cross-sectional area vs.  $x$  for various values of the time for (a)  $R = 0$  which pinches in the middle and (b)  $R = 10^{-2}$  which pinches at the end point. The initial condition is given by (4.8) with  $K = 10$ .

If  $\xi_p \in (0, 1)$ , then, since  $\xi_p$  is a minimum, we have  $p'(\xi_p) = 0$  and so  $p(\xi) = \tau_p + \frac{1}{2}p''(\xi_p)(\xi - \xi_p)^2 + O((\xi - \xi_p)^3)$ . At  $\tau = \tau_p$  (4.15) becomes

$$\frac{A^2}{\mathcal{H}} e^{-\mathcal{H}/A} = \frac{1}{2} e^{-\mathcal{H}/A_i(\xi_p) + \theta_i(\xi_p)} p''(\xi_p)(\xi - \xi_p)^2 + O((\xi - \xi_p)^3). \tag{4.17}$$

Therefore

$$A \rightarrow \frac{\mathcal{H}}{2 \ln |\xi - \xi_p|} \quad \text{as } \xi \rightarrow \xi_p \tag{4.18}$$

and the contribution to the extension (4.1) from the region that is close to the pinching point is integrable. A similar result can be obtained if  $\xi_p$  is located at one of the end points. Hence, the total extension will be finite even at pinching.

However, as the area tends to zero the velocity tends to infinity and so inertial terms will become important. The solution of (4.2)–(4.4) with non-zero inertia is shown in figure 4(b). Initially, the thread thins approximately uniformly until the minimum area becomes sufficiently small that inertia is important and prevents the thread from pinching at this location. As in the case without viscous heating, the inertia does not affect the end point and the area at the end point satisfies (4.13). Therefore, the thread will pinch at the end point at time

$$\tau_p = e^{-\theta_i(1)} \left[ A_i(1) - \mathcal{H} e^{\mathcal{H}/A_i(1)} E_1 \left( \frac{\mathcal{H}}{A_i(1)} \right) \right].$$

Using a similar calculation to that for  $\mathcal{H} = 0$ , we can see that the total extension will remain finite.

In figure 5 we show the result of pulling a thread that has an initial profile given by (4.8). We plot the minimum area and the area at the end of the thread against time for two different values of  $R$  and various values of  $\mathcal{H}$ . For the case with the larger inertia ( $R = 1$ ), the inertial effects prevent significant stretching in the middle of the thread and so the viscous heating plays a weak role. Ultimately, the thread will pinch at the end point where the inertia does not play a role and so viscous heating effects are important. For the case with weaker inertia ( $R = 0.1$ ), significant stretching occurs and initially cases with large viscous heating thin much more rapidly than those with

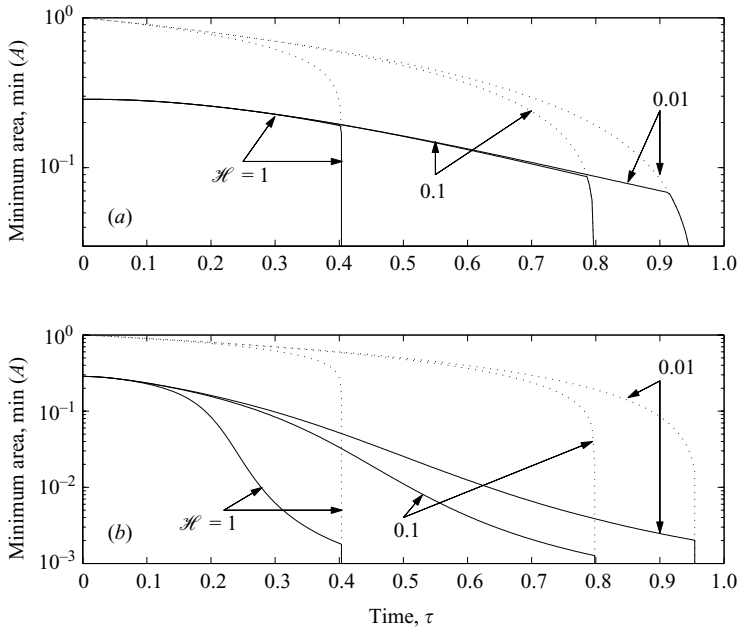


FIGURE 5. The minimum cross-sectional area vs. time for various values of  $\mathcal{H}$  for (a)  $R = 1$  and (b)  $R = 0.1$ . The initial condition is given by (4.8) with  $K = 10$ . The dotted line represents the cross-sectional area at the end point.

weak viscous heating. Ultimately, the thread will also pinch at the end point, but the thinning in the bulk is much greater than that for  $R = 1$ .

## 5. Discussion

We have considered the role played by viscous heating in controlling extensional flows of viscous threads. We have shown that even small amounts of viscous heating can lead to fundamental changes in the dynamics. For steady drawing, we have derived exact solutions for the case of zero inertia and have shown that there exists a critical pulling force above which inertialess solutions cannot exist. For pulling forces exceeding the critical value, the inclusion of inertia gives solutions that thin weakly over the bulk of the thread, but thin rapidly in a narrow region near the location where the pulling force is applied.

For an extending thread with zero inertia, we have derived exact solutions and shown that the total extension at pinching is infinite when viscous heating is neglected, but is finite when viscous heating is included. The location of pinch-off depends on the initial condition. However, if inertia is present, no matter how small, it will eventually become important and the thread will always pinch at the end where the force is applied. In all cases, viscous heating has a profound effect on the profile and can lead to very rapid thinning in the bulk of the thread.

J.J.W. was supported by a grant from the Research Grants Council of the Hong Kong Special Administrative Region, China [CityU 102705]. H.H. wishes to thank the Mathematics Department and LBJ Center at City University of Hong Kong. H.H. was supported in part by NSERC and MITACS.

## REFERENCES

- AL-MUBAIYEDH, U. A., SURESHKUMAR, R. & KHOMAMI, B. 2002 The effect of viscous heating on the stability of Taylor-Couette flow. *J. Fluid Mech.* **462**, 111–132.
- COSTA, A. & MACEDONIO, G. 2005 Viscous heating effects in fluids with temperature-dependent viscosity: triggering of secondary flows. *J. Fluid Mech.* **540**, 21–38.
- DEE, G. T. & SAUER, B. B. 1992 The molecular weight and temperature dependence of polymer surface tension: Comparison of experiment with interface gradient theory. *J. Colloid Interface Sci.* **152**, 85–103.
- DENN, M. M. 1980 Continuous drawing of liquids to form fibers. *Annu. Rev. Fluid Mech.*, **12**, 365–387.
- FITT, A. D., FURUSAWA, K., MONRO, T. M. & PLEASE, C. P. 2001 Modeling the fabrication of hollow fibers: Capillary drawing. *J. Lightwave Technol.* **19**, 1924–1931.
- FOREST, M. G., ZHOU, H. & WANG, Q. 2000 Thermotropic liquid crystalline polymer fibers. *SIAM J. Appl. Maths* **60**, 1177–1204.
- GALLACCHI, R., KOLSCH, S., KNEPPE, H. & MEIXNER, A. J. 2001 Well-shaped fibre tips by pulling with a foil heater. *J. Microscopy* **202**, 182–187.
- HUANG, H., MIURA, R. M., IRELAND, W. & PUIL, E. 2003 Heat-induced stretching of a glass tube under tension: Application to glass microelectrodes. *SIAM J. Appl. Maths* **63**, 1499–1519.
- KAYE, A. 1991 Convective coordinates and elongational flow. *J. Non-Newtonian Fluid Mech.* **40**, 55–77.
- MATSUMOTO, T. & BOGUE, D. C. 1978 Draw resonance involving rheological transitions. *Polym. Engng Sci.* **18**, 564–571.
- OCKENDON, H. 1979 Channel flow with temperature-dependent viscosity and internal viscous dissipation. *J. Fluid Mech.* **93**, 737–746.
- PEARSON, J. R. A. 1977 Variable-viscosity flows in channels with high heat-generation. *J. Fluid Mech.* **83**, 191–206.
- SCHOLZE, H. 1990 *Glass, Nature, Structure, and Properties*, translated by M. J. Lakin. Springer.
- STOKES, Y. M. & TUCK, E. O. 2004 The role of inertia in extensional flow of a viscous drop. *J. Fluid Mech.* **498**, 205–225.
- VASILYEV, O. V., TEN, A. A. & YUEN, D. A. 2001 Temperature-dependent viscous gravity currents with shear heating. *Phys. Fluids* **13**, 3664–3674.
- WHITE, J. M. & MULLER, S. J. 2002 Experimental studies on the stability of Newtonian Taylor-Couette flow in the presence of viscous heating. *J. Fluid Mech.* **462**, 133–159.
- WILSON, S. D. R. 1988 The slow dripping of a viscous fluid. *J. Fluid Mech.* **190**, 561–570.
- YIN, Z. & JALURIA, Y. 2000 Neck down and thermally induced defects in high-speed optical fiber drawing. *Trans. ASME: J. Heat Transfer* **122**, 351–362.